

---

# Effect of Transforming Growth Factor- $\beta$ on Osteoblast Cells Cultured on 3 Different Hydroxyapatite Surfaces

Joo L. Ong, PhD\*/David L. Carnes, PhD\*\*/A. Sogal, MS\*\*\*

In this study, the specific objective was to investigate the combined effect of different treatments of transforming growth factor- $\beta$  (TGF- $\beta$ ) and hydroxyapatite (HA) on osteoblast response in vitro. Since the nature of bone cell responses in vitro is influenced by the properties of HA ceramics, this study was divided into 2 components: a chemical and crystallographic characterization of the HA ceramics, and an in vitro cell culture study. Sintered HA samples were observed to have the highest crystallite size, compared to as-received HA and calcined HA samples. No differences in surface roughness and chemical composition were observed between the sintered, calcined, and as-received HA surfaces. In concurrence with the x-ray diffraction, high-resolution x-ray photoelectron spectroscopy of Ca 2p also indicated a higher crystallinity on sintered HA samples compared to calcined and as-received HA samples. Protein production by osteoblast cells was not statistically different on the 3 HA surfaces in the absence of TGF- $\beta$ . However, there was a dose-dependent increase in TGF- $\beta$ -stimulated protein production on the 3 different HA surfaces. As indicated by increased alkaline phosphatase-specific activity, as well as 1,25 (OH)<sub>2</sub> vitamin D<sub>3</sub>-stimulated osteocalcin production, a more differentiated osteoblastlike phenotype was observed on the sintered HA surfaces compared to the as-received HA and calcined HA surfaces. An increased osteoblast-like cell activity on sintered HA surfaces in the presence of different TGF- $\beta$  dosage suggested that sintering of HA surfaces may play an important role in governing cellular response.

(INT J ORAL MAXILLOFAC IMPLANTS 1999;14:217-225)

**Key words:** alkaline phosphatase activity, heat treatments, hydroxyapatite, osteocalcin concentration, transforming growth factor- $\beta$

---

**T**he study of tooth mineral has been linked to the investigation of calcium phosphate minerals, namely hydroxyapatite (HA). Like other bioactive materials, such as bioactive glass, HA has been shown to bond directly with bone, resulting in the formation of a uniquely strong bone-implant interface.<sup>1-4</sup> In spite of the desirable prop-

erties of HA, they are not strong enough for load-bearing areas.<sup>5-7</sup> Thus, in an attempt to improve osseointegration of implants in the bone and surrounding tissue, HA and other calcium phosphate ceramic coatings are being used.<sup>8</sup>

It is known that the surface properties of bio-material play critical roles in inducing a biologic response. Extensive in vivo research has demonstrated plasma-sprayed HA implants to be biocompatible, with reports of early skeletal attachment.<sup>9,10</sup> However, the nature of HA properties on tissue responses has not been fully investigated. A significantly higher osteogenesis level was observed in the presence of HA as compared to other biomaterials.<sup>11</sup> However, tissues respond differently to biomaterials of different crystallinity. Major differences in the adhesive response of epithelial cells to different crystallographic structures were reported,

---

\*Assistant Professor, University of Texas Health Science Center at San Antonio, Department of Restorative Materials, Division of Biomaterials, San Antonio, Texas.

\*\*Assistant Professor, University of Texas Health Science Center at San Antonio, Department of Endodontics, San Antonio, Texas.

\*\*\*Chief Engineer, CeraMed Corporation, Lakewood, Colorado.

**Reprint requests:** Dr Joo L. Ong, UTHSCSA, Division of Biomaterials, 7703 Floyd Curl Drive, San Antonio, Texas 78284. Fax: (210) 567-3669.

even though the chemical composition was identical.<sup>12</sup> In other studies observed, there was an adverse effect of amorphous HA coatings on the establishment of an interface with bone, whereas additional studies have suggested amorphous HA coatings to be advantageous for a more stable interface with the biologic environment.<sup>13-17</sup> It must also be noted that in many of these animal and clinical studies, the physical and chemical characteristics of plasma-sprayed HA were either unknown, poorly known, or left unstated.<sup>18</sup>

In addition to HA coatings, other surface modifications are employed as a means of controlling cellular responses to biomaterial surfaces. Currently, growth factors and cytokines are also being investigated as a means of stimulating desired cellular responses at the material-tissue interfaces. In addition, combinations of HA and such proteins as bone morphogenetic proteins have been proposed as a means to optimize bone-implant interactions.<sup>19</sup> In many instances, HA has been used as a carrier for the proteins.<sup>20</sup> Thus, the objective of this study was to investigate the combined effect of transforming growth factor- $\beta$  (TGF- $\beta$ ) and HA of different treatments on the osteoblast response *in vitro*.

### Materials and Methods

**Hydroxyapatite.** Hydroxyapatite disks were prepared by CeraMed Corporation (Lakewood, CO) using a wet reaction between calcium nitrate and ammonium phosphate. The HA precipitate was collected and washed several times with water. The HA paste was then dried in a spray dryer to obtain dry HA powders. The dry powders were then pressed into as-received HA disks (12 mm diameter by 2.5 mm thick) at a pressure of 20 kpsi. Calcined HA disks were obtained by calcining the as-received HA disks at 600°C over 4 hours, and sintered HA disks were produced by sintering the as-received HA disks (atmosphere pressure) at 1100°C over 7 hours. Materials characterization and *in vitro* cell culture experiments were then performed on the as-received, calcined, and sintered HA disks.

**Surface Roughness.** Surface roughness was measured using a profilometer (Taylor-Hobson Surtronic 3, Leicester, England). Three samples for each surface condition were measured, and the average roughness ( $R_a$ ) was quantified. Significant difference in the  $R_a$  values was statistically analyzed using analysis of variance (ANOVA). The alpha level for data analysis was set at  $\alpha = .05$ , and statistical differences were considered significant if  $P < .05$ .

**X-ray Diffraction.** Since the as-received, calcined, and sintered HA disks were from the same batch, only 1 HA sample from each treatment was examined using x-ray diffraction. The analyses were carried out on a Scintag (Model PAD V) diffractometer at 45 kV and 40 mA using copper  $K\alpha$  radiation. The diffractometer was equipped with a solid state detector and the diffraction pattern was collected as a continuous scan at 1.5 degrees/minute. Crystallite size was measured using the Rietveld technique. The technique was performed using a DBW Rietveld package (version 3.2, Georgia Institute of Technology, Atlanta, Georgia), with accuracy of  $\pm 25 \text{ \AA}$ .

**X-ray Photoelectron Spectroscopy.** Duplicate surfaces were analyzed in a Perkin-Elmer 5400 x-ray photoelectron spectroscopy (XPS) system (Physical Electronics, Eden Prairie, MN) using a base pressure of  $10^{-7}$  and a take-off angle of 45 degrees. Survey spectra were obtained over a range of 0 to 1100 eV using magnesium  $K\alpha$  radiation at 15 kV and 20 mA. A pass energy of 89.54 eV was used to collect the survey spectra. Atomic concentrations for all identified elements were quantified from the spectra taken at a pass energy of 17.9 eV, using tabulated elemental sensitivity factors obtained from the XPS system. High-resolution spectra of the C 1s, Ca 2p and P 2p were collected with a pass energy of 8.95 eV. From the high-resolution spectra, full width at half maximum (FWHM) for Ca 2p<sub>1/2</sub> and Ca 2p<sub>3/2</sub> were measured. Photoelectron peak positions were corrected for charging by reference to the adventitious C 1s peak at  $284.6 \pm 0.4$  eV. All high-resolution spectra were deconvoluted using the Gaussian-Lorentzian model. The calcium:phosphate ratios of as-received, calcined, and sintered HA surfaces were statistically compared using ANOVA, and statistical differences were considered significant at  $P < .05$ .

**Cell Culture.** Bone cell activity studies were carried out using mature rat osteoblast cell line (ROS 17/2.8). The cells were seeded onto the HA disks in 24 well-culture plates at a density of 10,000 cells/cm<sup>2</sup>/mL in alpha-minimal essential media ( $\alpha$ -MEM) containing 7% fetal bovine serum, 1% antibiotic-antimycotic solution (5000 units penicillin, 5000 mg streptomycin, 250 mg/mL amphotericin  $\beta$  [Gibco, Life Technologies, Grand Island, NY]), 50  $\mu$ g/mL ascorbic acid, and 4 mmol/L  $\beta$ -glycerophosphate. The study was conducted in an incubator at 37°C and a humidified atmosphere of 95% air and 5% CO<sub>2</sub>. The culture medium was changed every 2 days with complete  $\alpha$ -MEM media. At confluency, the cells were stimulated

with 0, 0.01, 0.1, and 1 ng/mL TGF- $\beta$  (R & D Systems, Minneapolis, MN). Seven days after stimulation, triplicate samples from each treatment were assayed for protein synthesis, alkaline phosphatase activity, and osteocalcin production.

**Cell Surface and Matrix-Associated Protein Synthesis.** Total cell surface and matrix-associated protein synthesis was measured using the Pierce bicinchoninic acid (BCA) protein assay (Pierce, Rockford, IL). On the day of the assay, media were removed from the cell culture and the cell layers were lysed with 1 mL of Triton X-100 (0.2%, Sigma, St Louis, MO). An aliquot of the triton lysate (30  $\mu$ L) was added to 200  $\mu$ L of BCA working reagent and the samples were incubated for 30 minutes at 37°C. The concentration of cell surface and matrix-associated protein synthesized was determined from the absorbance read by a microplate reader at 570 nm, using a standard protein concentration curve. The concentration of proteins on HA disks of different treatment were statistically compared using ANOVA, and statistical differences were considered significant at  $P < .05$ .

**Alkaline Phosphatase-Specific Assay.** On the day of the assay, medium was removed from the cell cultures and the cell layers were lysed with 1 mL triton X-100 (0.2%). An aliquot of the triton lysate (50  $\mu$ L) was added to 50  $\mu$ L of working reagent containing equal parts of 1.5 mol/L 2-amino-2-methyl-1-propanol (Sigma), 20 mmol/L p-nitrophenyl phosphate (Sigma), and 1 mmol/L magnesium chloride. The samples were then incubated for 1 hour at 37°C. After incubation, the reaction was stopped with 100  $\mu$ L of 1 N sodium hydroxide and the absorbance read at 410 nm using a microplate reader. Alkaline phosphatase (ALP) activity was determined from the absorbance using a standard curve prepared from p-nitrophenol stock standard (Sigma). The ALP-specific activity was statistically compared using ANOVA, and statistical differences were considered significant at  $P < .05$ .

**1,25 (OH)<sub>2</sub> Vitamin D<sub>3</sub>-stimulated Osteocalcin Production.** On the day of the assay, the medium was removed from the cultures and frozen at -20°C until assayed. The samples were then lyophilized using a speed-vac (Savant, Holbrook, NY). The sample residues were reconstituted at 1/4 of the original starting volume using glass-distilled water. 1,25 (OH)<sub>2</sub> D<sub>3</sub>-stimulated osteocalcin production was then measured using a commercially available rat osteocalcin radioimmunoassay kit (Biomedical Technologies, MA). Differences in 1,25 (OH)<sub>2</sub> D<sub>3</sub>-stimulated osteocalcin production were statistically compared using ANOVA, and statistical differences were considered significant at  $P < .05$ .

## Results

**Surface Roughness.** The as-received, calcined, and sintered HA surfaces were observed to have a mean  $R_a$  value ( $\pm$  SEM) of  $0.67 \pm 0.07 \mu\text{m}$ ,  $0.80 \pm 0.07 \mu\text{m}$ , and  $0.67 \pm 0.07 \mu\text{m}$ , respectively. At an  $\alpha$  level of .05, it was observed that the surface roughness of as-received, calcined, and sintered HA surfaces was not significantly different.

**X-ray Diffraction.** X-ray diffraction analyses for all HA samples indicated an HA-type structure, with as-received HA samples having broad HA peaks (Fig 1). Calcined and sintered HA samples (Figs 2 and 3) displayed more distinct, sharper x-ray diffraction peaks as compared to as-received HA samples, indicating higher crystallinity. The crystallite size of sintered HA samples exceeds 2500 Å and is different from the crystallite size of calcined HA (275 Å) and as-received HA (200 Å) samples.

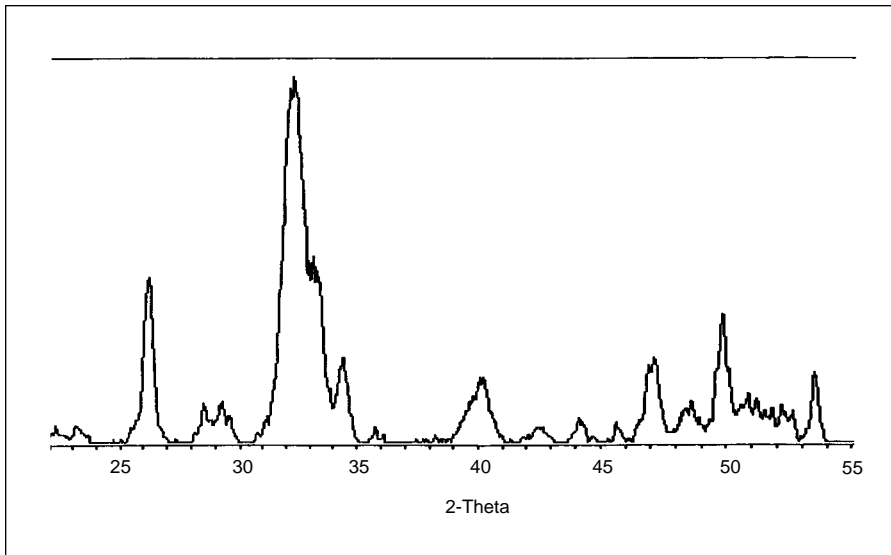
**X-ray Photoelectron Spectroscopy.** A representative XPS spectrum of HA surfaces is provided in Fig 4. Carbon (7 - 16 atomic %), phosphorus, oxygen, and calcium were observed on all HA surfaces, with no statistical difference in the calcium:phosphorus ratio observed between the HA surfaces (Table 1). No statistical difference in the calcium:phosphorus ratio of as-received, calcined, and sintered HA surfaces was observed.

Figure 5 shows a typical P 2p spectrum observed on all HA samples. Curve-fitted P 2p spectra indicated 2 peaks for all HA samples. All HA samples were observed to have a component at  $132.7 \pm 0.2 \text{ eV}$  and a smaller component at  $133.7 \pm 0.2 \text{ eV}$ .

Similarly, the morphology of Ca 2p spectrum was similar for all HA samples. A typical high-resolution Ca 2p spectrum is shown in Fig 6. The Ca 2p spectrum observed on all HA surfaces was a doublet, with Ca 2p<sub>3/2</sub> and Ca 2p<sub>1/2</sub> at  $346.9 \pm 0.2 \text{ eV}$  and  $350.4 \pm 0.2 \text{ eV}$ , respectively. However, as shown in Table 2, the full width at half maximum (FWHM) of the Ca 2p<sub>3/2</sub> and Ca 2p<sub>1/2</sub> was significantly different, depending on the treatments.

**Cell Surface and Matrix-Associated Protein.** In the absence of TGF- $\beta$  stimulation, no statistical difference in protein production was observed for cells cultured on sintered, calcined, and as-received HA surfaces (Fig 7). However, at a concentration of 1 ng/mL TGF- $\beta$ , the cells cultured on sintered HA surfaces exhibited significantly higher total cell surface and matrix-associated protein when compared to either as-received or calcined HA surfaces.

**Alkaline Phosphatase-Specific Activity.** When compared to the as-received and calcined HA



**Fig 1** X-ray diffraction of the as-received HA samples, showing data collected from 22 degrees to 55 degrees  $2\theta$ .

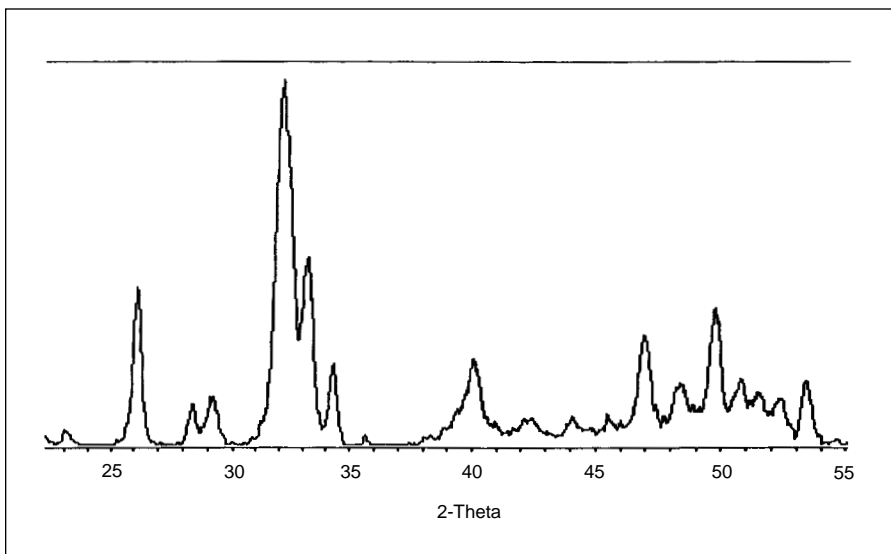


**Fig 2** X-ray diffraction of the calcined HA samples, showing data collected from 22 degrees to 55 degrees  $2\theta$ .

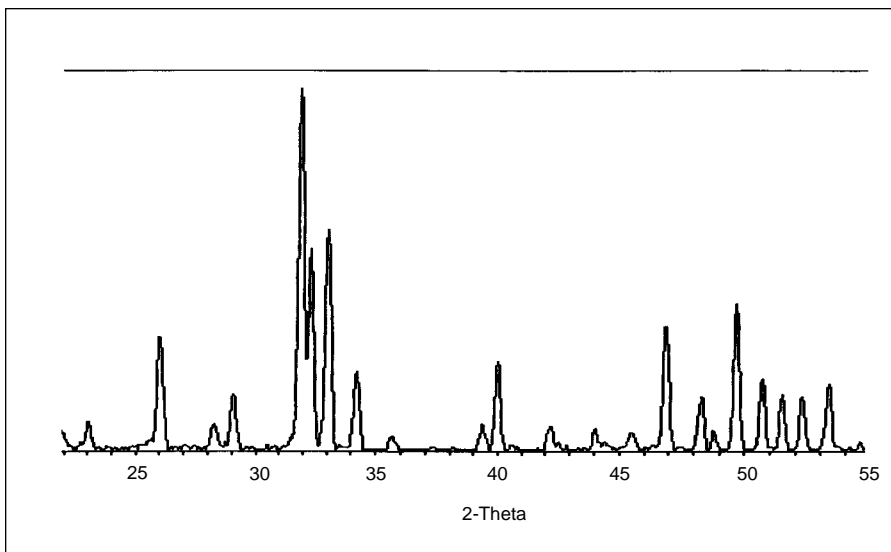


**Fig 3** X-ray diffraction of the sintered HA samples, showing data collected from 22 degrees to 55 degrees  $2\theta$ .

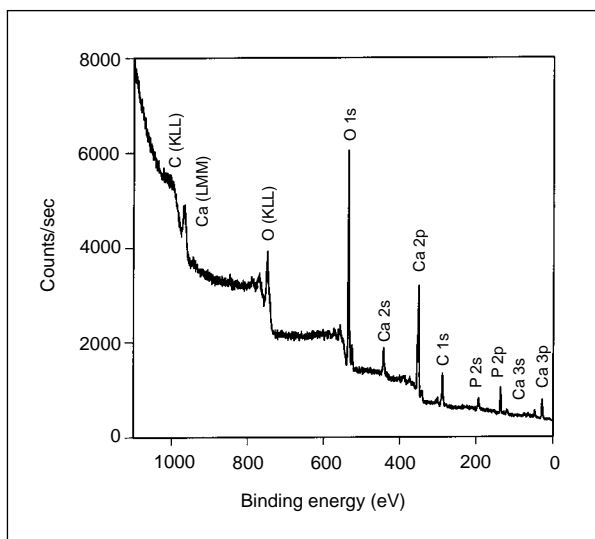


**Fig 4** A representative XPS spectrum of the as-received, calcined, and sintered HA surfaces.

**Table 1** Average Calcium:Phosphate Ratio ( $\pm 1$  Standard Error) on HA Surfaces of Different Treatments

Sample	Calcium:phosphate ratio
As-received	$1.6 \pm 0.1$
Calcined	$1.63 \pm 0.1$
Sintered	$1.75 \pm 0.1$

**Table 2** Full Width at Half Maximum of Ca 2p Peaks ( $\pm 1$  Standard Error) on HA Surfaces of Different Treatments

Sample	Ca 2p <sub>3/2</sub>	Ca 2p <sub>1/2</sub>
As-received	$1.67 \pm 0.12$	$1.75 \pm 0.12$
Calcined	$1.61 \pm 0.08$	$1.68 \pm 0.08$
Sintered	$1.40 \pm 0.11$	$1.42 \pm 0.11$

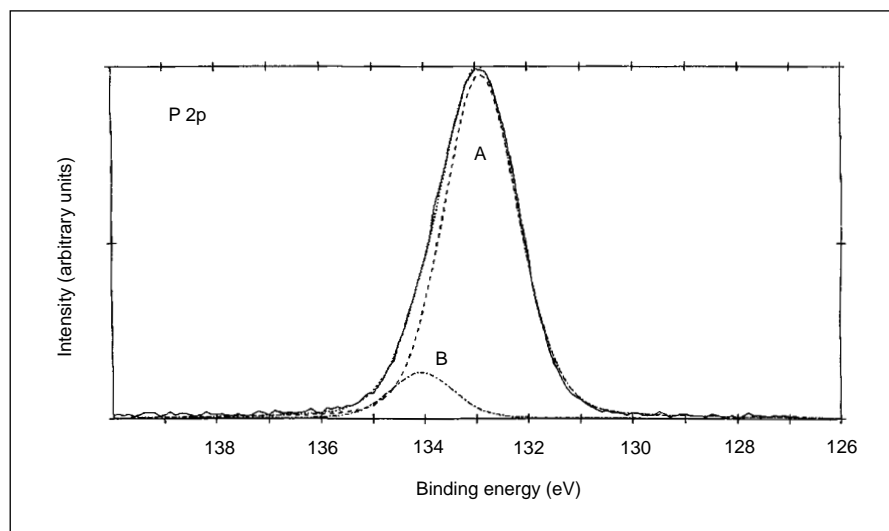


**Fig 5** A representative high-resolution XPS spectrum for P 2p. Component A is at  $132.7 \pm 0.2$  eV and component B is at  $133.7 \pm 0.2$  eV.

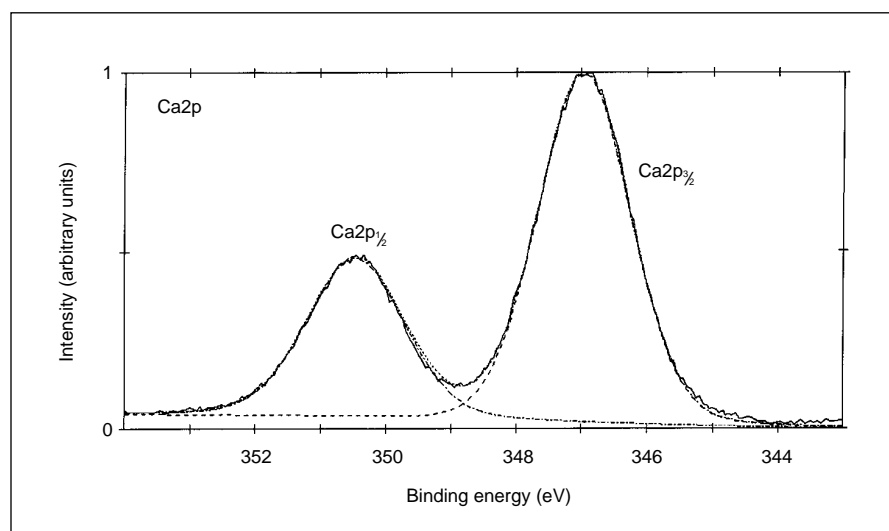


**Fig 6** A representative high-resolution XPS spectrum of Ca 2p showing the Ca 2p<sub>3/2</sub> and Ca 2p<sub>1/2</sub>.

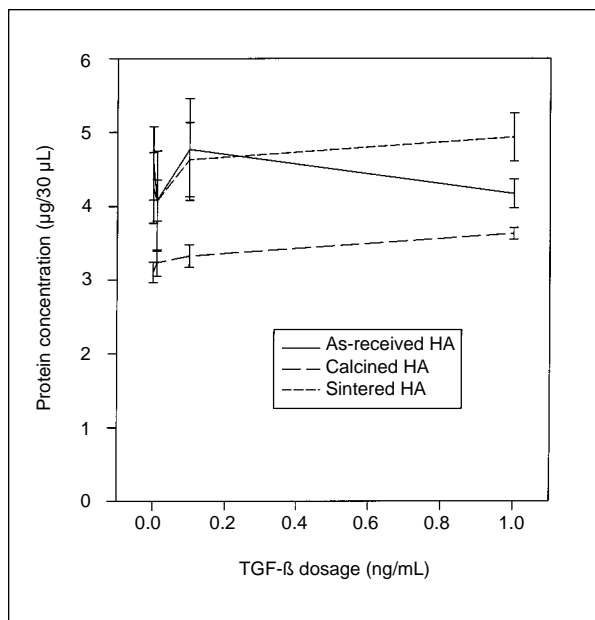


**Fig 7** Cell layer and matrix-associated protein synthesis by ROS 17/2.8 cells on HA surfaces of different treatments. Error bar represents 1 standard error.

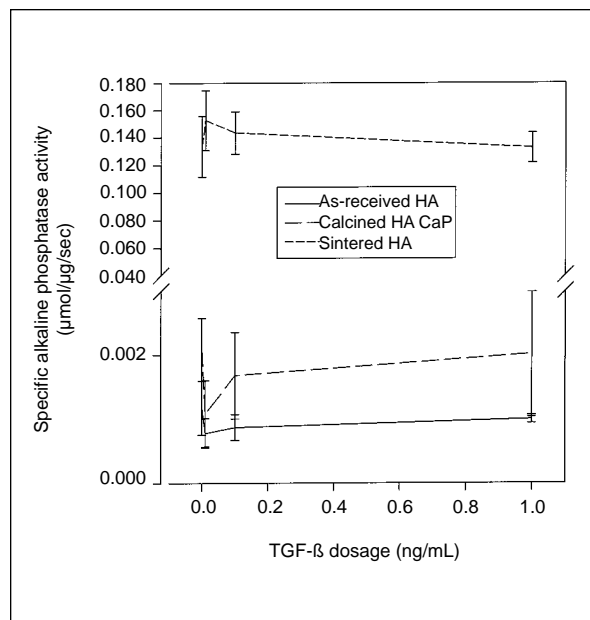


**Fig 8** Alkaline phosphatase-specific activity of ROS 17/2.8 cells on HA surfaces of different treatments. Error bar represents 1 standard error.

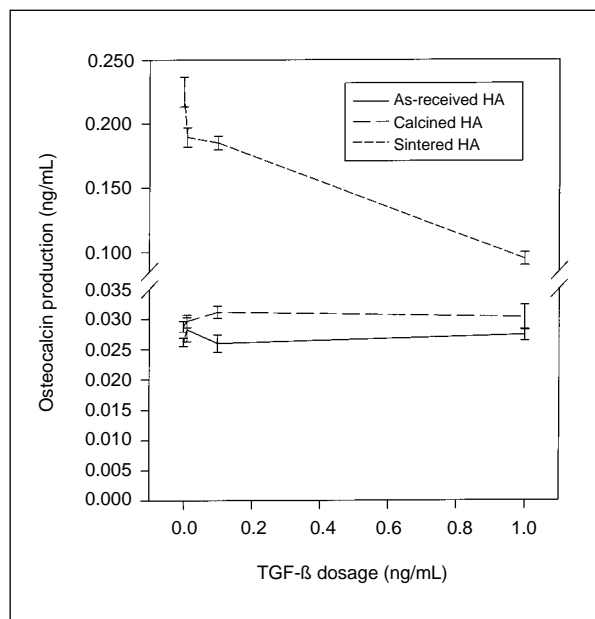


**Fig 9** 1,25 (OH<sub>2</sub>) vitamin D<sub>3</sub>-stimulated osteocalcin production by ROS 17/2.8 cells on HA surfaces of different treatments. Error bar represents 1 standard error.

surfaces, the rat osteoblast sarcoma (ROS) 17/2.8 cells cultured on sintered HA surfaces exhibited significantly higher ALP-specific activity for all TGF-β concentrations tested (Fig 8). The level of ALP-specific activity of cells cultured on the as-received and calcined HA surfaces did not statistically change over the different TGF-β concentrations evaluated.

**1,25 (OH<sub>2</sub>) Vitamin<sub>3</sub>-Stimulated Osteocalcin Production.** As shown in Fig 9, no statistical difference in 1,25 (OH<sub>2</sub>) vitamin D<sub>3</sub>-stimulated osteocalcin production was observed for cells grown on the as-received and calcined HA surfaces at different TGF-β concentrations. Similar to the ALP-specific activity, a statistically higher 1,25 (OH<sub>2</sub>) vitamin D<sub>3</sub>-stimulated osteocalcin production was observed for cells grown on sintered HA. However, the osteocalcin production of cells cultured on sintered HA surfaces was observed to decrease when the TGF-β concentration was increased to 1 ng/mL.

### Discussion

Depending on the properties of biomaterials, different rates of cellular responses have been observed in vitro.<sup>21-24</sup> These differences have been attributed to varying surface chemistries and crystallinities. Using a profilometer in this study, the authors observed that the surface roughness of as-

received, calcined, and sintered HA surfaces was not significantly different, suggesting that the treatment does not affect surface roughness.

As shown in this study, the x-ray diffraction analyses of calcined and sintered HA samples displayed sharper and more distinct x-ray diffraction peaks as compared to as-received HA samples, indicating higher crystallinity. The crystallite size of sintered HA samples exceeded 2,500 Å and was different from the crystallite size of calcined HA (275 Å) and as-received HA (200 Å) samples. A crystallite size of about 5,000 Å has been reported for HA powders.<sup>25,26</sup> These differences in crystallite size have been associated with varying degrees of dissolution rates, with smaller, more imperfect crystals being subject to greater dissolution.<sup>27-29</sup> The increase in crystallite size during sintering concurs with observations made by other investigators.<sup>30</sup> Other studies using high-resolution transmission electron microscopy have shown that higher annealing temperature not only increases grain size but also improves crystal perfection by minimizing the number or preventing the formation of crystal void defects.<sup>31</sup> As the grains become larger, the gaps between grains shrink and the material becomes denser.

As observed from the XPS analyses, no statistical difference in the calcium:phosphate ratio of as-received, calcined, and sintered HA surfaces was observed. Curve-fitting the P 2p spectra of all HA samples indicated the presence of a major component at  $132.7 \pm 0.2$  eV and a smaller component at  $133.7 \pm 0.2$  eV. The 132.7 eV component was attributed to the presence of phosphate species and the 133.7 eV component was attributed to the presence of hydrogen phosphate species.<sup>32,33</sup> Similarly, the morphology of Ca 2p spectrum was similar for all HA samples. However, as shown in Table 2, the FWHM of the Ca 2p<sub>3/2</sub> and Ca 2p<sub>1/2</sub> was significantly different, depending on the treatments. The FWHM of Ca 2p spectrum for sintered HA was statistically smaller compared to the calcined and as-received HA samples. The change in FWHM of Ca 2p was attributed to differences in crystallinity. As observed in other biomaterials of different crystallinities, changes in FWHM were also observed when comparing amorphous TiO<sub>2</sub> on Ti surfaces (FWHM = 1.3) to the TiO<sub>2</sub> single crystal (FWHM = 1.1).<sup>34,35</sup>

In *in vitro* cell culture studies, protein synthesis is an important marker for evaluating cell function. Matrix proteins in bone have been reported to play a crucial role in the calcification and architectural construction of these hard tissues.<sup>36</sup> In this study, total cell surface and matrix associated pro-

tein of the ROS 17/2.8 cells cultured on sintered, calcined, and as-received HA surfaces were not statistically different in the absence of TGF-β stimulation (Fig 7). However, there is a dose-dependent increase in TGF-β stimulated protein production by cells on the 3 different HA surfaces. At a concentration of 1 ng/mL, protein production on the sintered HA surfaces was observed to be statistically higher than protein production on calcined and as-received HA surfaces. With an increase in TGF-β stimulation, a significantly greater protein level was observed for the ROS 17/2.8 cells grown on sintered HA surfaces, suggesting a possible influence of heat treatments of HA surfaces on protein synthesis.

Two other biochemical markers, the ALP-specific activity and osteocalcin level, are used as markers for determining osteoblast phenotype and are considered to be important factors in determining bone mineralization (Harris MA, personal communication).<sup>37-39</sup> As shown in Figs 8 and 9, cells grown on the sintered HA surfaces were observed to exhibit significantly higher ALP-specific activity and 1,25 (OH)<sub>2</sub> vitamin D<sub>3</sub>-stimulated osteocalcin production at all concentrations of TGF-β used in this study, when compared to the as-received and calcined HA surfaces, indicating a higher cellular differentiation and mineralized matrix production on sintered HA surfaces. However, as shown in Fig 9, the 1,25 (OH)<sub>2</sub> vitamin D<sub>3</sub>-stimulated osteocalcin production was observed to decrease significantly as the dosage of TGF-β increased, suggesting the arrest of the mineralization phase in the presence of increased TGF-β level. This finding was supported by other *in vivo* studies, which showed a negative correlation between TGF-β dosage and ingrowth distance of bone and tissues, with an increased TGF-β level increasing the inhibition of bone and tissue growth.<sup>20</sup>

No statistical difference in ALP-specific activity and 1,25 (OH)<sub>2</sub> vitamin D<sub>3</sub>-stimulated osteocalcin production was observed when cells were cultured on as-received and calcined HA surfaces. The low ALP-specific activity and 1,25 (OH)<sub>2</sub> vitamin D<sub>3</sub>-stimulated osteocalcin production on as-received and calcined HA surfaces was suggested to be attributed to many factors, including the affinity of proteins to HA surfaces of different treatments, the ingestion of HA particles, and intracellular solubilization.<sup>40,41</sup> It was observed that intracellular dissolution of calcium-containing crystals greatly influenced cell behavior.<sup>42-44</sup> The presence of HA particles and its intracellular solubilization were hypothesized to adversely affect

calcium and phosphate homeostatic mechanisms and to modify the mechanical regulators of DNA synthesis without any evidence of cytotoxic effect.<sup>45</sup> Further studies are required to confirm this hypothesis.

### Conclusions

Overall, this study has shown the importance of characterizing HA surfaces. As indicated by x-ray diffraction and XPS, sintered HA surfaces exhibited the largest crystallite size compared to as-received and calcined HA surfaces. No differences in the surface roughness and chemical composition were observed between any of the HA surfaces. In the presence of different levels of TGF- $\beta$ , a higher level of ALP-specific activity, total cell surface and matrix-associated protein, and 1,25 (OH)<sub>2</sub> vitamin D<sub>3</sub>-stimulated osteocalcin production were observed for ROS 17/2.8 cells cultured on sintered HA surfaces, suggesting a more differentiated, osteoblast-like phenotype when compared to cells cultured on as-received and calcined HA surfaces. The osteoblast-like phenotype displayed by the cells cultured on sintered HA surfaces suggests that the combined presence of TGF- $\beta$  on HA surfaces of different treatments may play an important role in governing the expression of osteoblast characteristics.

### Acknowledgment

This study was supported by the Whitaker Foundation and CeraMed Corporation.

### References

- Hench LL, Andersson O. Bioactive glasses. In: Hench LL, Wilson J (eds). *An Introduction of Bioceramics*, Advance Series in Ceramics, vol 1. London: World Scientific, 1993:41–73.
- Hench LL, Wilson J. Surface active materials. *Biomater Sci* 1984;226:630–636.
- Hench LL, Splinter RJ, Allen WC, Greenlee TK. Bonding mechanisms at the interface of ceramic prosthetic materials. *J Biomed Mater Res* 1971;2:117–141.
- Osborn JF, Newesely H. The material science of calcium phosphate ceramics. *Biomaterials* 1980;1:108–111.
- De Groot K, Wolke JGC, Jansen JA. State of the art: Hydroxylapatite coatings for dental implants. *J Oral Implantol* 1994;20:232–234.
- Jarcho M. Retrospective analysis of hydroxyapatite development for oral implant applications. *Dent Clin North Am* 1991;36:16–26.
- Kay J. Calcium phosphate coatings for dental implants: Current status and future potential. *Dent Clin North Am* 1992;36:1–18.
- Herman H. Plasma-spray deposition processes. *MRS Bull* 1988;12:60–67.
- Rivero DP, Fox J, Skipor AK, Urban RM, Galante JO. Calcium phosphate-coated porous titanium implants for enhanced skeletal fixation. *J Biomed Mater Res* 1988; 22:191–201.
- Bloebaum RD, Merrell M, Gustke K, Simmons M. Retrieval analysis of a hydroxyapatite-coated hip prosthesis. *Clin Orthop Rel Res* 1991;267:97–102.
- Iwano T, Kurosawa H, Shibuya K, Kawahara H. Osteogenesis of bone marrow cells with hydroxyapatite in diffusion chambers. In: Vincenzi P (ed). *Ceramics in Substitutive and Reconstructive Surgery*. Amsterdam: Elsevier, 1991: 323–328.
- Hanein D, Sabanay H, Addadi L, Geiger B. Selective interactions of cells with crystal surfaces. *J Cell Sci* 1993;104:275–288.
- Dhert WJA, Klein CPAT, Wolke JGC, van der Velde EA, de Groot K, Rozing PM. Fluorapatite-, magnesiumwhitlockite-, and hydroxyapatite-coated titanium plugs: Mechanical bonding and the effect of different implantation sites. In: Vincenzi P (ed). *Ceramics in Substitutive and Reconstructive Surgery*. Amsterdam: Elsevier, 1991:385–394.
- Gabbi C, Borghetti P, Cacchioli A, Antoletti N, Pitteri S. Physical, chemical, and biological characterization of hydroxyapatite coatings of differentiated crystallinity. *Trans 4th World Biomater Congr* 1992;5.
- Maxian SH, Zawadski JP, Dunn MG. Evaluation of amorphous versus crystalline hydroxyapatite coatings on smooth and rough titanium: In vitro and in vivo studies. *Trans 4th World Biomater Congr* 1992;101.
- Van Blitterswijk CA, Leenders H, van der Brink J, Bovell Y, Flach J, de Bruijn J, de Groot K. Degradation and interface reactions of hydroxyapatite coatings: Effect of crystallinity. *Trans 19th Ann Meeting Soc Biomater* 1993;337.
- De Bruijn JD, Klein CPAT, de Groot K, van Blitterswijk CA. Influence of crystal structure on the establishment of the bone calcium phosphate interface in vitro. *Cells Mater* 1993;3:407–417.
- Larson FG. Hydroxyapatite coatings for medical implants. *Med Dev Diag Industry* 1994;April:34–40.
- Ono I, Gunji H, Suda K, Kaneko F, Murata M, Saito T, Kuboki Y. Bone induction of hydroxyapatite covered with bone morphogenetic protein and covered with periosteum. *Plast Reconstr Surg* 1995;95:1265–1272.
- Aspenberg P, Jepsson C, Wang JS, Bostrom M. Transforming growth factor beta and bone morphogenetic protein 2 for bone ingrowth: A comparison using bone chambers in rats. *Bone* 1996;19:499–503.
- Grinnell F. Cellular adhesiveness and extracellular substrata. *Int Rev Cytol* 1978;53:65.
- Ben-Ze'ev A. Animal cell shape changes and gene expression. *Bioessays* 1991;13:207–212.
- Bale MD, Wolfahrt LS, Mosher DF, Tomasini B, Sutton RC. Identification of vitronectin as a major plasma protein adsorbed on polymer surfaces of different copolymer composition. *Blood* 1989;2698–2706.
- Hattori S, Andrade JD, Hibbs JB, Gregonis DE, King RN. Fibroblast cell proliferation of charged hydroxyethyl methacrylate copolymers. *J Coll Int Sci* 1985;104:73–78.
- Koch B, Wolke JGC, de Groot K. X-ray diffraction studies on plasma-sprayed calcium phosphate-coated implants. *J Biomed Mater Res* 1990;24:665–667.
- Maxian SH, Zawadsky JP, Dunn MG. In vitro evaluation of amorphous calcium phosphate and poorly crystallized hydroxyapatite coatings on titanium implants. *J Biomed Mater Res* 1993;27:111–117.



27. LeGeros RZ. Calcium phosphate materials in restorative dentistry. A review. *Adv Dent Res* 1988;2:164-180.
28. Thompson DD, Posner AS, Laughlin WS, Blumenthal NC. Comparison of bone apatite in osteoporotic and normal Eskimos. *Calcif Tissue Int* 1983;25:392-393.
29. Hurson S, Laceyfield W, Lucas L, Ong J, Whitehead R, Bumgardner J. Effect of the crystallinity of plasma sprayed HA coatings on dissolution. *Trans 19th Ann Meeting Soc Biomater* 1993;223.
30. Jarcho M, Bolen CH, Thomas MB, Bobick J, Kay JF, Doremus RH. Hydroxylapatite synthesis and characterization in dense polycrystalline form. *J Mater Sci Mater Med* 1976;11:2027-2035.
31. Daculsi G, LeGeros RZ, LeGeros JP, Mitre D. Lattice defects in calcium phosphate ceramics: High resolution TEM ultrastructural study. *J Appl Biomater* 1991;2:147-152.
32. Hanawa T, Ota M. Calcium phosphate naturally formed on titanium in electrolyte solution. *Biomaterials* 1991;12:767-774.
33. Ong JL, Lucas LC, Raikar GN, Connatser R, Gregory JC. Spectroscopic characterization of passivated titanium in a physiologic solution. *J Mater Sci Mater Med* 1995;6:113-119.
34. Bange K, Ottermann CR, Anderson O, Jeschkowski U, Laube M, Feile R. Investigation of TiO<sub>2</sub> films deposited by different techniques. *Thin Solid Films* 1991;197:279-285.
35. Sayers CN, Armstrong NR. X-ray photoelectron spectroscopy of TiO<sub>2</sub> and other titanate electrodes and various standard titanium oxide materials: Surface compositional changes of the TiO<sub>2</sub> electrode during photoelectrolysis. *Surf Sci* 1978;77:301-320.
36. Glimcher MJ. Mechanism of calcification: role of collagen fibrils and collagen-phosphoprotein complexes in vitro and in vivo. *Anat Rec* 1989;224:139-153.
37. Price PA. Vitamin K-dependent formation of bone Gla protein (osteocalcin) and its function. *Vitam Horm* 1985;42:65-108.
38. Hauschka PV, Reid ML. Timed appearance of a calcium-binding protein for normal chick egg hatchability. *Science* 1978;201:835-837.
39. Nakashima M, Nagasawa H, Yamada Y, Reddi AH. Regulatory role transforming growth factor-beta, bone morphogenetic protein-2, and protein-4 on gene expression of extracellular matrix proteins and differentiation of dental pulp cells. *Dev Biol* 1994;162:18-28.
40. Herr G, Wahl D, Kusswetter W. Osteogenic activity of bone morphogenetic protein and hydroxyapatite composite implants. *Ann Chir Gynaecol* 1993;207(suppl):99-107.
41. Alliot-Licht B, Gregoire M, Orly I, Menanteau J. Cellular activity of osteoblasts in the presence of hydroxyapatite: An in vitro experiment. *Biomaterials* 1991;12:752-756.
42. Chung HS, McCarty DJ. Mitogenesis induced by calcium-containing crystals. *Exp Cell Res* 1985;157:63-70.
43. Gregoire M, Orly I, Kerebel LM, Kerebel B. In vitro effects of calcium phosphate biomaterials on fibroblastic cell behavior. *Biol Cell* 1987;59:255-260.
44. Orly I, Gregoire M, Menanteau J, Dard M. Effect of synthetic calcium phosphates on the <sup>3</sup>H-thymidine incorporation and alkaline phosphatase activity of human fibroblasts in culture. *J Biomed Mater Res* 1989;23:1433-1440.
45. Kozawa O, Takatsuki K, Kotake K, Yoneda M, Oiso Y, Saito H. Possible involvement of protein kinase C in proliferation and differentiation of osteoblast-like cells. *Fed Eur Biochem Soc* 1989;243:183-185.